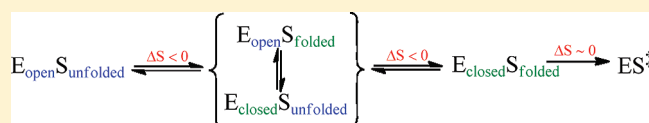


Entropic and Enthalpic Components of Catalysis in the Mutase and Lyase Activities of *Pseudomonas aeruginosa* PchB

Qianyi Luo, Kathleen M. Meneely, and Audrey L. Lamb\*

Molecular Biosciences, University of Kansas, Lawrence, Kansas 66045, United States

**ABSTRACT:** The isochorismate-pyruvate lyase from *Pseudomonas aeruginosa* (PchB) catalyzes two pericyclic reactions, demonstrating the eponymous activity and also chorismate mutase activity. The thermodynamic parameters for these enzyme-catalyzed activities, as well as the uncatalyzed isochorismate decomposition, are reported from temperature dependence of  $k_{\text{cat}}$  and  $k_{\text{uncat}}$  data. The entropic effects do not contribute to enzyme catalysis as expected from previously reported chorismate mutase data. Indeed, an entropic penalty for the enzyme-catalyzed mutase reaction ( $\Delta S^\ddagger = -12.1 \pm 0.6 \text{ cal}/(\text{mol K})$ ) is comparable to that of the previously reported uncatalyzed reaction, whereas that of the enzyme-catalyzed lyase reaction ( $\Delta S^\ddagger = -24.3 \pm 0.2 \text{ cal}/(\text{mol K})$ ) is larger than that of the uncatalyzed lyase reaction ( $-15.77 \pm 0.02 \text{ cal}/(\text{mol K})$ ) documented here. With the assumption that chemistry is rate-limiting, we propose that a reactive substrate conformation is formed upon loop closure of the active site and that ordering of the loop contributes to the entropic penalty for converting the enzyme substrate complex to the transition state.



## ■ INTRODUCTION

The isochorismate-pyruvate lyase (PchB) from *Pseudomonas aeruginosa* catalyzes an asynchronous [1,5]-sigmatropic shift with a hydrogen transfer from C2 to C9 that has been shown to have a pericyclic transition state: the enzyme-catalyzed reaction shows quantitative transfer of the C2 hydrogen and a  $^2\text{H}$  kinetic isotope effect consistent with the elimination reaction<sup>1</sup> (Figure 1A). PchB also exhibits chorismate mutase (CM) activity (Figure 1B), which is a pericyclic reaction, albeit more than 2 orders of magnitude less efficient than physiological chorismate mutases.<sup>2,3</sup> Therefore, this enzyme performs two related pericyclic reactions in a single active site with a considerable difference in efficiency.

PchB is neither structurally nor functionally homologous to the pyruvate lyases of other shikimic acid metabolites.<sup>4–6</sup> Instead, PchB shares homology with the chorismate mutases of the AroQ structural class, including *Escherichia coli* chorismate mutase (EcCM).<sup>7</sup> EcCM is actually the N-terminal domain of a two-domain multifunctional prephenate dehydratase that was cloned separately and purified.<sup>8</sup> The structure of EcCM reveals an intertwined dimer of three helices each with two equivalent buried active sites composed of residues from each subunit.<sup>9</sup> A transition state analogue (TSA) is bound in the active site, oriented by arginine residues that align the carboxylates. In contrast, the chorismate mutase from *Bacillus subtilis* (BsCM) is a member of the AroH structural class, and is a trimer which forms a pseudo- $\alpha\beta$ -barrel with three equivalent active sites at the subunit interfaces. The same TSA is bound in one of the solved structures, and is oriented in the active site by comparable arginines.<sup>10,11</sup> Apo- and prephenate-bound structures of BsCM have also been completed.<sup>10,12</sup> Despite the overall structural differences between the two classes, the active sites of EcCM and BsCM are usually considered comparable due to their shape and charge complementarity.<sup>13</sup>

Less is known about the structures of the chorismate mutases from *Klebsiella pneumoniae* (KpCM; formerly *Aerobacter aerogenes*)

and *Streptomyces aureofaciens* (SaCM), as the original work was completed on enzyme purified from bacterial culture.<sup>14</sup> A BLAST<sup>15</sup> search reveals that *K. pneumoniae* has a prephenate dehydratase analogous to EcCM, and an alignment reveals that the CM domains share 92% sequence identity (all sequence comparisons were calculated using L-ALIGN<sup>16</sup>). Early work suggested two CM active sites,<sup>14</sup> so we will classify this enzyme as a member of the AroQ family. *S. aureofaciens*, in contrast, contains a monofunctional chorismate mutase that shares sequence homology to BsCM (38% identity, 64% similarity). SaCM was originally thought to have two or four subunits per oligomer,<sup>14</sup> but in recent work, the calculations have assumed trimeric enzyme.<sup>17</sup> We will classify this enzyme as a member of the AroH family.

There has been the assertion that the enzyme-catalyzed chorismate mutase reaction is entropically driven,<sup>14,18</sup> though this is a matter of debate.<sup>17</sup> This hypothesis is proposed from temperature dependence of  $k_{\text{cat}}$  data from both structural classes of chorismate mutases. We report herein the thermodynamic parameters, entropic and enthalpic contributions to the free energy of activation, for both the lyase and mutase reactions of PchB, and for the uncatalyzed lyase reaction, and compare these data to those reported previously for the AroQ and AroH chorismate mutases.

## ■ MATERIALS AND METHODS

**Protein Preparation.** Wild-type PchB without a histidine tag was prepared as previously described.<sup>7</sup>

**Preparation of Isochorismate and Chorismate.** Isochorismate was isolated from *K. pneumoniae* 62-1 harboring the *entC* plasmid pKS3-02<sup>19</sup> with only minor changes, as described previously.<sup>3</sup>

Received: March 7, 2011

Published: April 19, 2011

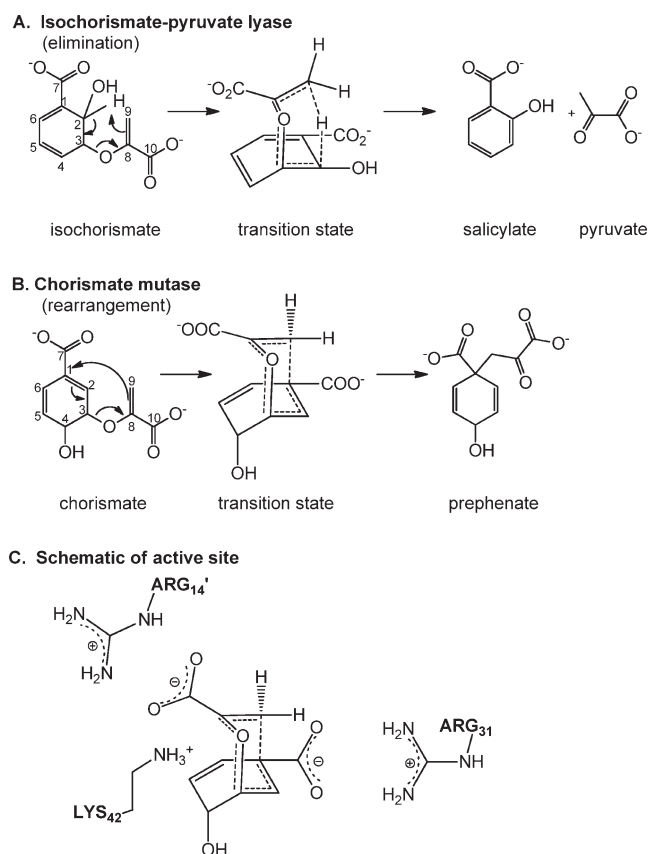


Figure 1

Chorismate (Sigma, 60–80% pure) was recrystallized as previously described.<sup>20</sup>

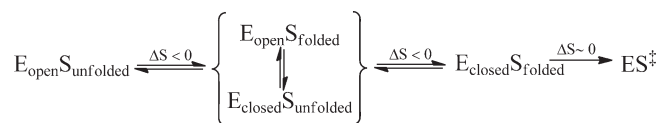
**Chorismate Mutase (CM) Activity Assays.** Initial velocities were measured in 50 mM sodium/potassium phosphate buffer pH 7.5 at temperatures from 5 to 45 °C by measuring chorismate disappearance at 310 nm with a Cary 50 Bio spectrophotometer (Varian) and an electrothermal single cell holder for temperature control ( $\pm 0.1$  °C). Enzyme (80  $\mu$ M) was incubated for 10 min at the desired temperature, and the reaction was initiated by the addition of chorismate, varied in concentration from 0.05 to 1.4 mM. Kinetic data were fit to the Michaelis–Menten equation by the nonlinear regression function of KaleidaGraph (Synergy Software).

**Isochorismate-Pyruvate Lyase (IPL) Activity Assays.** Initial velocities were measured in 50 mM sodium/potassium phosphate buffer pH 7.5 at temperatures from 5 to 45 °C by measuring the accumulation of salicylate by fluorescence with an excitation wavelength of 300 nm and an emission wavelength of 430 nm using a Cary Eclipse fluorescence spectrophotometer (Varian) and an electrothermal single cell holder for temperature control ( $\pm 0.1$  °C). Enzyme (0.25  $\mu$ M) was incubated for 10 min at the desired temperature, and the reaction was initiated by the addition of isochorismate, varied in concentration from 2 to 32  $\mu$ M. Kinetic data were fit to the Michaelis–Menten equation by the nonlinear regression function of KaleidaGraph (Synergy Software).

**Calculation of Thermodynamic Activation Parameters.** The activation enthalpy ( $\Delta H^\ddagger$ ) and entropy ( $\Delta S^\ddagger$ ) were determined from the linear regression of the data collected from 5 to 45 °C according to the Eyring equation:<sup>21</sup>

$$k_{\text{cat}} = \left( \frac{k_B T}{h} \right) e^{-[(\Delta H^\ddagger/RT) - (\Delta S^\ddagger/R)]}$$

Scheme 1



where  $k_B$  is Boltzmann's constant,  $h$  is Planck's constant,  $R$  is the ideal gas constant, and  $T$  is the temperature in Kelvin.

#### Uncatalyzed Decomposition of Isochorismate in Solution.

Isochorismate undergoes elimination to form salicylate and pyruvate and rearrangement to form isoprephenate in the absence of enzyme.<sup>22</sup> Salicylate formation was monitored in water at temperatures from 30 to 70 °C by monitoring fluorescence with an excitation wavelength of 310 nm and an emission wavelength of 430 nm using a Cary Eclipse fluorescence spectrophotometer (Varian) and an electrothermal single cell holder for temperature control ( $\pm 0.1$  °C). The amount of salicylate formed was determined with a standard curve (0–50  $\mu$ M). The rate of isochorismate disappearance ( $k$ ) was determined from the plot of salicylate formation ( $y$ ) versus time ( $t$ ) according to the equation:

$$y = a(1 - e^{-kt})$$

where  $a = I_0(k_1/k)$ ,  $k = k_1 + k_2$ , and  $I_0 = 350$   $\mu$ M (the initial isochorismate concentration).  $k_1$  is the rate for the elimination reaction and  $k_2$  is the rate for the Claisen rearrangement. Thermodynamic activation parameters for the elimination and rearrangement reactions were calculated from the corresponding Eyring plots.

## RESULTS AND DISCUSSION

**Model for the Entropic Contribution to the Transition from the Enzyme–Substrate Complex to the Transition State.** The experiments described here and those from previous work used for comparison all report the temperature dependence of  $k_{\text{uncat}}$  or  $k_{\text{cat}}$ . These data therefore reflect changes in free energy, enthalpy, and entropy for converting the free substrate ( $S$ ) to the free transition state ( $S^\ddagger$ ) in the case of  $k_{\text{uncat}}$  or the enzyme substrate complex ( $ES$ ) to the transition state ( $ES^\ddagger$ ) in the case of  $k_{\text{cat}}$ . The entropic component for formation of the  $ES^\ddagger$  for the reactions discussed range from an equal or larger penalty than that observed for the uncatalyzed reaction to very small, and in one case, within experimental error of zero. We propose that in the former instance, where the entropic penalty is large, there is an enzyme conformational change that is concomitant with the organization of the substrate (Scheme 1). In this case, the binding event does not necessarily organize (or fold) the substrate nor does the loop or lid over the active site close. Instead, this occurs in subsequent steps which incur an entropic penalty. In the enzymes for which the entropic contribution to the  $ES$  to  $ES^\ddagger$  transition is small or negligible, the substrate and enzyme are preorganized by the binding event. In other words, the binding event folds the substrate and closes the loop or lid over the active site.

**Chorismate Mutase Reaction.** In solution, chorismate goes from a very mobile reactant state ( $S$ ) to a more ordered transition state ( $S^\ddagger$ ) for conversion of chorismate to prephenate, and this change has a  $\Delta S^\ddagger$  value of  $-12.9$  cal/(mol K)<sup>23</sup> (Table 1). When unfolded, the substrate is solvated in a variety of ways, including structured waters surrounding the hydrophobic expanse. These structured waters are lost to bulk solvent upon substrate folding providing a positive change in entropy which is offset wholly or

Table 1. Comparison of the Thermodynamic Parameters for the Mutase and Lyase Reactions

| activity  | $\Delta G^\ddagger$ (kcal/mol) | $\Delta H^\ddagger$ (kcal/mol) | $\Delta S^\ddagger$ (cal/(mol K)) | structural family |
|---|--------------------------------|--------------------------------|-----------------------------------|-------------------|
| chorismate $\rightarrow$ prephenate                           |                                |                                |                                   |                   |
| Uncatalyzed rearrangement <sup>b</sup>                        | 24.5                           | 20.7 $\pm$ 0.4                 | −12.9 $\pm$ 0.4                   |                   |
| PchB CM <sup>c</sup>  | 19.53 $\pm$ 0.01               | 15.9 $\pm$ 0.2                 | −12.1 $\pm$ 0.6                   | AroQ              |
| <i>B. subtilis</i> CM <sup>d</sup>                            | 15.4                           | 12.7 $\pm$ 0.4                 | −9.1 $\pm$ 1.2                    | AroH              |
| <i>E. coli</i> CM <sup>e</sup>                                | 17.2                           | 16.3 $\pm$ 0.5                 | −3.0 $\pm$ 1.6                    | AroQ              |
| <i>S. aureofaciens</i> CM <sup>f</sup>                        | 15.0                           | 14.5 $\pm$ 0.4                 | −1.6 $\pm$ 1.1                    | AroH              |
| <i>K. pneumoniae</i> CM <sup>f</sup>                          | 16.2                           | 15.9 $\pm$ 0.4                 | −1.1 $\pm$ 1.2                    | AroQ              |
| chorismate $\rightarrow$ <i>p</i> -hydroxybenzoate + pyruvate |                                |                                |                                   |                   |
| Uncatalyzed elimination <sup>b</sup>                          | 25.7                           | 23.6 $\pm$ 2.8                 | −6.9 $\pm$ 1.5                    |                   |
| isochorismate $\rightarrow$ isoprephenate                     |                                |                                |                                   |                   |
| Uncatalyzed rearrangement <sup>g</sup>                        | 25.04 $\pm$ 0.03               | 23.48 $\pm$ 0.06               | −5.22 $\pm$ 0.01                  |                   |
| isochorismate $\rightarrow$ salicylate + pyruvate             |                                |                                |                                   |                   |
| Uncatalyzed elimination <sup>g</sup>                          | 25.90 $\pm$ 0.02               | 21.19 $\pm$ 0.03               | −15.77 $\pm$ 0.02                 |                   |
| PchB IPL <sup>g</sup>   | 18.47 $\pm$ 0.03               | 11.2 $\pm$ 0.1                 | −24.3 $\pm$ 0.2                   | AroQ              |

<sup>a</sup>  $\Delta G^\ddagger$  calculated at 298.15 K. <sup>b</sup> Andrews et al.<sup>23</sup> <sup>c</sup> Figure 2. <sup>d</sup> Kast et al.<sup>17</sup> <sup>e</sup> Galopin et al.<sup>18</sup> <sup>f</sup> Gorisch et al.<sup>14</sup> <sup>g</sup> Figure 4.

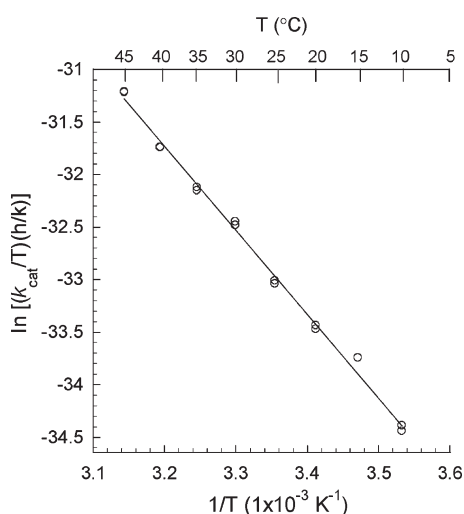


Figure 2. Temperature dependence of  $k_{\text{cat}}$  for the chorismate mutase reaction of PchB (○).

partly by negative changes in entropy arising from the restrictions imposed in folding of the substrate and from solvation of the developing delocalized charge of the transition state which is not present in the ground state. Therefore, the observed negative entropy of activation for the uncatalyzed reaction is a combination of the effects of such changes as substrate folding, release of structured waters, and solvation of developing charges.

For the enzymatic conversion of chorismate to prephenate, the *K. pneumoniae* and *S. aureofaciens* mutases demonstrate a small change for the conversion from the enzyme–substrate complex to the transition state (−1.1, −1.6 cal/(mol K), respectively).<sup>14</sup> It has been argued that the observation of little entropic change from ES to ES<sup>‡</sup> indicates that the chorismate is prearranged in the active site and only becomes slightly more ordered during this step of the reaction cycle.<sup>14</sup> The *E. coli* chorismate mutase demonstrates a  $\Delta S^\ddagger$  value of −3.0 cal/(mol K),<sup>18</sup> which is within error of the *K. pneumoniae* and *S. aureofaciens* mutase values.<sup>14</sup> These three enzymes are therefore considered to be classic entropy traps: the enzyme achieves the conformational constriction of the substrate during formation of the ES so that conversion of ES to ES<sup>‡</sup> incurs no large entropic

penalty.<sup>14,24</sup> The *B. subtilis* mutase has  $\Delta S^\ddagger$  value which is more similar to the uncatalyzed reaction than to the other chorismate mutases (−9.1 cal/(mol K)),<sup>17</sup> leading to the suggestion that the active site exerts less conformational control and overcomes this deficit with a more significant change in enthalpy.<sup>17</sup> This compensation allows for the similar  $\Delta G^\ddagger$  values for all four mutases (15.0–17.2 kcal/mol). The temperature dependence of  $k_{\text{cat}}$  for the chorismate mutase activity of PchB (Figure 2), on the other hand, gives a  $\Delta S^\ddagger$  value of −12.1 cal/(mol K), which is within experimental error of the  $\Delta S^\ddagger$  value of the uncatalyzed reaction. By the same argument, this result suggests that there is no conformational control of the substrate in the active site upon formation of the enzyme–substrate complex. This is contrary to structural biology data,<sup>3,7</sup> which clearly show that the carboxylates of ligands in the active site are oriented by arginines (Figure 1C). Nevertheless, the data here indicate that the differing protein folds (AroQ versus AroH) do not correlate to the differing conformational control of the substrate in the ES complex. Instead, these data corroborate the idea that these active sites are indeed comparable and structural differences do not explain the relative entropic and enthalpic contributions.

**Isochorismate-Pyruvate Lyase Reaction.** In solution, isochorismate spontaneously undergoes a Claisen rearrangement to form isoprephenate, which undergoes further reaction to form 3-carboxyphenylpyruvate through the loss of a water molecule (Figure 3). Isochorismate also spontaneously forms salicylate and pyruvate in the elimination reaction. Using an NMR assay and measuring the formation of isoprephenate, 3-carboxyphenylpyruvate, salicylate and pyruvate, Hilvert and colleagues have previously experimentally determined the  $\Delta G^\ddagger$  values for the uncatalyzed reactions at 333.15 K, 24.8 and 26.2 kcal/mol, respectively.<sup>22</sup> In the experiments presented here, the uncatalyzed elimination reaction was monitored by measuring increasing salicylate fluorescence allowing for the calculation of the concomitant rearrangement reaction (Figure 4A), and the thermodynamic parameters were determined as described in the Materials and Methods (Table 1). The  $\Delta G^\ddagger$  values reported in Table 1 are calculated for 298.15 K for direct comparison to the previously reported chorismate mutase values. The  $\Delta G^\ddagger$  values for the uncatalyzed reaction calculated for 333.15 K are in good agreement with the  $\Delta G^\ddagger$  values from Hilvert, with the uncatalyzed rearrangement  $\Delta G^\ddagger$  value of 25.2 kcal/mol and the elimination  $\Delta G^\ddagger$  value of 26.4 kcal/mol, but the enthalpic and entropic contributions are somewhat unexpected. We had expected

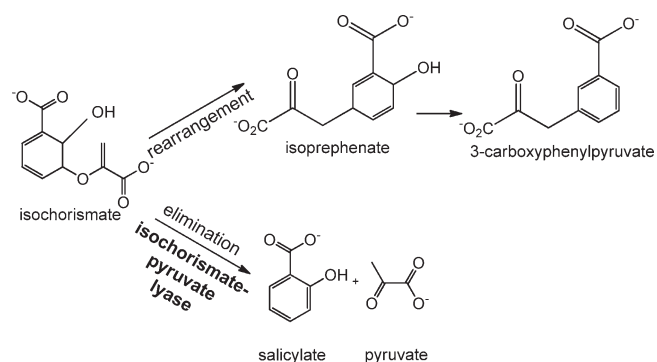


**Figure 3.** Thermal decomposition of isochorismate. Reaction catalyzed by PchB in bold.

enthalpic and entropic contributions for these reactions to be comparable to those previously reported for the mutase reaction (Table 1). However, the entropic penalty for the isochorismate rearrangement contributes considerably less ( $-5.22$  cal/(mol K)) than that for the chorismate rearrangement ( $-12.9$  cal/(mol K)),<sup>23</sup> whereas the entropic contribution of the uncatalyzed isochorismate elimination reaction is the most significant ( $-15.77$  cal/(mol K)). Indeed, the entropic penalty for the isochorismate elimination is most similar to that of the chorismate rearrangement ( $-12.9$  cal/(mol K)). The thermodynamic parameters of the physiological lyase activity of PchB are the most surprising (Figure 4B). This reaction is clearly enthalpically driven, and has a very large entropic penalty ( $-24.3$  cal/(mol K)), which is more than 1.5-fold greater than that of the uncatalyzed reaction ( $-15.77$  cal/(mol K)).

**Rate-Determining Step.** Previous work to determine the rate-determining step for the chorismate mutases comes from several different protein forms and from many different kinds of experiments, with the weight of the evidence favoring a chemistry step that is largely or wholly rate-limiting. First, primary heavy atom isotope effects documented for the independent EcCM domain<sup>25,26</sup> and BsCM<sup>25</sup> were consistent with the hypothesis that chemistry is significantly rate-limiting. Second, the effects of viscosogens on steady-state parameters indicate that EcCM is insensitive to changes in viscosity and thus chemistry is fully rate-determining, whereas BsCM showed kinetic parameters that were decreased significantly with increasing glycerol and chemistry was calculated to be  $\sim 60$ – $70\%$  rate-determining.<sup>27</sup> The only caveat is that the uncatalyzed reaction showed a 15% secondary tritium kinetic isotope effect at C3 and C9, whereas no comparable effect was detected for the enzyme-catalyzed reaction of the chorismate mutase-prephenate dehydrogenase (the bifunctional enzyme of which one domain is a chorismate mutase with 23% identity and 46% similarity to EcCM).<sup>28</sup> If interpreted in isolation, this would suggest that some physical step is rate-determining. It would be intriguing to learn if this is also true of the EcCM domain from the dehydratase enzyme.

**The Contribution of Loop or Lid Closing to Catalysis.** Hur and Bruce concluded from molecular dynamics simulations of EcCM initiated at the loop-closed ES conformer that “...the loop structure at residues 42–48 fluctuates more in the [transition state] than in the [enzyme–substrate complex],” which led to the argument that the active site is *less* stable at the transition state and promotes the idea of a “near attack conformation” for catalysis.<sup>29</sup> In other words, it was argued that the substrate and enzyme are preorganized by formation of the ES and formation of the transition state is inconsequential for catalysis. The theoretical calculations of Skolaski and colleagues

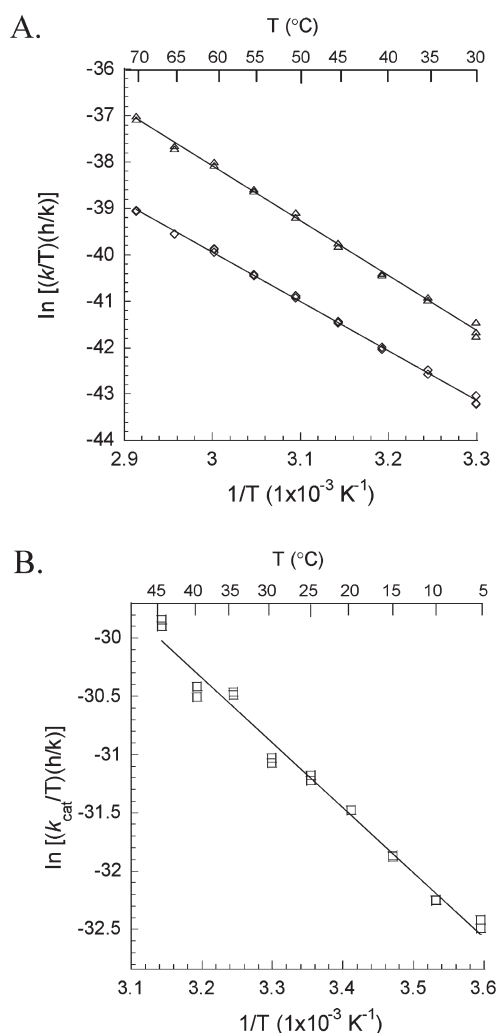


**Figure 4.** Isochorismate-pyruvate lyase. (A) Temperature dependence of the uncatalyzed isochorismate elimination reaction ( $\diamond$ ) and the uncatalyzed isochorismate rearrangement reaction ( $\triangle$ ). (B) Temperature dependence of  $k_{\text{cat}}$  for the isochorismate-pyruvate lyase reaction of PchB ( $\square$ ).

suggest that Arg90 of BsCM (comparable to the lysine of the active site loop in the AroQ enzymes) has the greatest stabilization effect and is responsible (with Arg7) for the preorganization effects of the substrate.<sup>30,31</sup> NMR relaxation dynamics of BsCM showed little movement at Arg90, which is found in a  $\beta$ -strand.<sup>32</sup> However, these data indicate that the C-terminus serves as a lid and there is substantial ordering of flexible residues upon ligand binding.<sup>32</sup> PchB shows a dramatic change in the active site between the apo- and ligand-bound structures with a disorder-to-order transition of the loop,<sup>3,7</sup> promoting the hypothesis that active site loop dynamics are important for catalysis. These combined data for both the AroH and AroQ enzymes suggest that loop or lid movement is involved in the catalytic cycle and should be considered in entropic models for catalysis. In agreement with this idea, changes to less negative values of  $\Delta S^\ddagger$  have been attributed to decreasing phosphate gripper loop size in orotidine 5'-monophosphate decarboxylases,<sup>33</sup> suggesting that active site loop mobility contributes to observed entropy changes for conversion of the enzyme–substrate complex to the transition state.

**Conclusions.** With the predominance of evidence indicating that chemistry is rate-limiting and evidence for a conformational

change in the loop or lid closing the active site, we propose the model shown in Scheme 1. Since the reactant state for  $k_{\text{cat}}$  is the enzyme–substrate complex, a reactive conformation of the substrate may not be formed upon binding of substrate to the enzyme ( $E_{\text{open}}S_{\text{unfolded}}$ ). Instead, the conformer for catalysis ( $E_{\text{closed}}S_{\text{folded}}$ ) is formed along the reaction coordinate approaching the transition state ( $ES^{\ddagger}$ ), or in line with classical transition state theory, the reactive substrate conformation is formed at the transition state. The ordering of substrate and loop therefore both contribute to the large entropic penalty for the overall ES to  $ES^{\ddagger}$  transition. These substrate and loop ordering steps may be sequential as shown in the scheme, or may be concerted: closing of the active site loop may force the substrate into its folded form for catalysis. For the chorismate mutase reactions with no entropic penalty for the ES to  $ES^{\ddagger}$  transition, substrate binding may promote closing of the active site (forming  $E_{\text{closed}}S_{\text{folded}}$ ), and therefore, the entropy change for this transition is approximately zero.

## AUTHOR INFORMATION

### Corresponding Author

lamb@ku.edu

## ACKNOWLEDGMENT

We are grateful to T. C. Gamblin for spectrometer use and R. L. Schowen for insightful discussions. This publication was made possible by funds from the Kansas Masonic Cancer Research Institute, by NIH award number P20 RR016475 from the INBRE Program of the National Center for Research Resources, and by NIH award number R01 AI77725 from the National Institute for Allergy and Infectious Disease.

## ABBREVIATIONS

AroH, chorismate mutase structural family of which BsCM is a member; AroQ, chorismate mutase structural family of which EcCM is a member; BsCM, *Bacillus subtilis* chorismate mutase; CM, chorismate mutase; EcCM, *E. coli* chorismate mutase; ES, enzyme–substrate complex;  $ES^{\ddagger}$ , transition state of enzyme-catalyzed reaction; IPL, isochorismate-pyruvate lyase; KpCM, *Klebsiella pneumoniae* chorismate mutase; PchB, isochorismate-pyruvate lyase from *Pseudomonas aeruginosa*;  $S^{\ddagger}$ , transition state of uncatalyzed reaction; SaCM, *Streptomyces aureofaciens* chorismate mutase; TSA, transition state analogue.

## REFERENCES

- (1) DeClue, M. S.; Baldrige, K. K.; Kunzler, D. E.; Kast, P.; Hilvert, D. *J. Am. Chem. Soc.* **2005**, *127*, 15002–15003.
- (2) Gaille, C.; Kast, P.; Haas, D. *J. Biol. Chem.* **2002**, *277*, 21768–21775.
- (3) Luo, Q.; Olucha, J.; Lamb, A. L. *Biochemistry* **2009**, *48*, 5239–5245.
- (4) Gallagher, D. T.; Mayhew, M.; Holden, M. J.; Howard, A.; Kim, K. J.; Vilker, V. L. *Proteins* **2001**, *44*, 304–311.
- (5) Nakai, T.; Mizutani, H.; Miyahara, I.; Hirotsu, K.; Takeda, S.; Jhee, K. H.; Yoshimura, T.; Esaki, N. *J. Biochem.* **2000**, *128*, 29–38.
- (6) Spraggon, G.; Kim, C.; Nguyen-Huu, X.; Yee, M. C.; Yanofsky, C.; Mills, S. E. *Proc. Natl. Acad. Sci. U.S.A.* **2001**, *98*, 6021–6026.
- (7) Zaitseva, J.; Lu, J.; Olechowski, K. L.; Lamb, A. L. *J. Biol. Chem.* **2006**, *281*, 33441–33449.
- (8) Stewart, J.; Wilson, D. B.; Ganem, B. *J. Am. Chem. Soc.* **1990**, *112*, 4582–4584.

- (9) Lee, A. Y.; Karplus, P. A.; Ganem, B.; Clardy, J. *J. Am. Chem. Soc.* **1995**, *117*, 3627–3628.
- (10) Chook, Y. M.; Gray, J. V.; Ke, H.; Lipscomb, W. N. *J. Mol. Biol.* **1994**, *240*, 476–500.
- (11) Chook, Y. M.; Ke, H.; Lipscomb, W. N. *Proc. Natl. Acad. Sci. U.S.A.* **1993**, *90*, 8600–8603.
- (12) Ladner, J. E.; Reddy, P.; Davis, A.; Tordova, M.; Howard, A. J.; Gilliland, G. L. *Acta Crystallogr.* **2000**, *D56*, 673–683.
- (13) Lee, A. Y.; Stewart, J. D.; Clardy, J.; Ganem, B. *Chem. Biol.* **1995**, *2*, 195–203.
- (14) Gorisch, H. *Biochemistry* **1978**, *17*, 3700–3705.
- (15) Camacho, C.; Coulouris, G.; Avagyan, V.; Ma, N.; Papadopoulos, J.; Bealer, K.; Madden, T. L. *BMC Bioinf.* **2009**, *10*, 421.
- (16) Huang, X.; Miller, W. *Adv. Appl. Math.* **1991**, *12*, 373–381.
- (17) Kast, P.; Asif-Ullah, M.; Hilvert, D. *Tetrahedron Lett.* **1996**, *37*, 2691–2694.
- (18) Galopin, C. C.; Zhang, S.; Wilson, D. B.; Ganem, B. *Tetrahedron Lett.* **1996**, *37*, 8675–8678.
- (19) Schmidt, K.; Leistner, E. *Biotech. Bioeng.* **1995**, *45*, 285–291.
- (20) Rieger, C. E.; Turnbull, J. L. *Prep. Biochem. Biotechnol.* **1996**, *26*, 67–76.
- (21) Connors, K. A. *Chemical Kinetics. The Study of Reaction Rates in Solution*; Wiley-VCH Publishers: New York, 1990.
- (22) DeClue, M. S.; Baldrige, K. K.; Kast, P.; Hilvert, D. *J. Am. Chem. Soc.* **2006**, *128*, 2043–2051.
- (23) Andrews, P. R.; Smith, G. D.; Young, I. G. *Biochemistry* **1973**, *12*, 3492–3498.
- (24) Westheimer, F. H. *Adv. Enzymol. Rel. Areas Mol. Biol.* **1962**, *24*, 441–482.
- (25) Gustin, D. J.; Mattei, P.; Kast, P.; Wiest, O.; Lee, L.; Cleland, W. W.; Hilvert, D. *J. Am. Chem. Soc.* **1999**, *121*, 1756–1757.
- (26) Wright, S. K.; DeClue, M. S.; Mandal, A.; Lee, L.; Wiest, O.; Cleland, W. W.; Hilvert, D. *J. Am. Chem. Soc.* **2005**, *127*, 12957–12964.
- (27) Mattei, P.; Kast, P.; Hilvert, D. *Eur. J. Biochem.* **1999**, *261*, 25–32.
- (28) Addadi, L.; Jaffe, E. K.; Knowles, J. R. *Biochemistry* **1983**, *22*, 4494–4501.
- (29) Hur, S.; Bruice, T. C. *Proc. Natl. Acad. Sci. U.S.A.* **2002**, *99*, 1176–1181.
- (30) Szeftczyk, B.; Claeysens, F.; Mulholland, A. J.; Sokalski, W. A. *Int. J. Quantum Chem.* **2007**, *107*, 2274–2285.
- (31) Szeftczyk, B.; Mulholland, A. J.; Ranaghan, K. E.; Sokalski, W. A. *J. Am. Chem. Soc.* **2004**, *126*, 16148–16159.
- (32) Eletsky, A.; Kienhofer, A.; Hilvert, D.; Pervushin, K. *Biochemistry* **2005**, *44*, 6788–6799.
- (33) Toth, K.; Amyes, T. L.; Wood, B. M.; Chan, K. K.; Gerlt, J. A.; Richard, J. P. *Biochemistry* **2009**, *48*, 8006–8013.